Article

Ab Initio Research on a New Type of Half-Metallic Double Perovskites, A_2CrMO_6 (A = IVA Group Elements; M = Mo, Re and W)

Yun-Ping Liu [1], Huei-Ru Fuh [2] and Yin-Kuo Wang [3],*

[1] Department of Physics, National Taiwan Normal University, Taipei 106, Taiwan;
  E-Mail: viva.guitarra@gmail.com
[2] Graduate Institute of Applied Physics, National Taiwan University, Taipei 106, Taiwan;
  E-Mail: c4491141@gmail.com
[3] Center for General Education and Department of Physics, National Taiwan Normal University, Taipei 106, Taiwan

* Author to whom correspondence should be addressed; E-Mail: kant@ntnu.edu.tw;
  Tel.: +886-2-7734-1130.

Abstract: The research based on density functional theory was carried out using generalized gradient approximation (GGA) for full-structural optimization and the addition of the correlation effect (GGA + U (Coulomb parameter)) in a double perovskite structure, $A_2BB'O_6$. According to the similar valance electrons between IIA(s^2) and IVA(p^2), IVA group elements instead of alkaline-earth elements settled on the A-site ion position with fixed BB' combinations as CrM (M = Mo, Re and W). The ferrimagnetic half-metallic (HM-FiM) properties can be attributed to the *p-d* hybridization between the Cr$_d$-M_p and the double exchange. All the compounds can be half-metallic (HM) materials, except Si_2CrMoO_6, Ge_2CrMo and Ge_2CrReO_6, because the strong-correlation correction should be considered. For M = W, only A = Sn and Pb are possible candidates as HM materials. Nevertheless, an examination of the structural stability is needed, because Si, Ge, Sn and Pb are quite different from Sr. All compounds are stable, except for the Si-based double perovskite structure.

Keywords: *ab-initio* research; half-metallic; double perovskites

1. Introduction

Transition metals are discovered to possess high Curie temperature in a research study on an ordered double perovskite material, $A_2BB'O_6$ [1]. The *A*-site elements are alkaline-earth ions, such as Ca, Sr, Ba and *B*, *B'* being [2] the large low-field tunneling magneto resistance (TMR) [3] at room temperature and half-metallicity [4]. The earliest half-metallic (HM) compound, denoted as Sr_2FeMoO_6 [4–8], was found by Kobayashi *et al*. Half-metallic (HM) materials are metallic for one spin direction, while they act as an insulator for the other spin direction [9–14]. Thus, three characteristic properties can be found: (1) 100% spin polarization at the Fermi level; (2) quantization of the magnetic moment; and (3) a spin susceptibility of zero. HM materials with this interesting attribute can be used as computer memory, magnetic recorders, and so on.

Ordered double perovskites, $A_2BB'O_6$, are a good baseline structure for determining suitable HM material candidates, because there are a variety of combinations for substituting the *A*-site or *B*-site elements. In previous research, HM compounds were found, such as Sr_2FeWO_6 [6], $Sr_2FeReO6$ [15,16], $Sr_2MnMoO6$ [16], Sr_2CuOsO_6 [17], Sr_2VOsO_6 [18], Sr_2NiRuO_6 [19], Sr_2FeTiO_6 [20], Sr_2CrMoO_6 [12,21], Sr_2CoMoO_6 [12], Sr_2CrReO_6 [11,15] and Sr_2CrWO_6 [14,22] for the same ion Sr on the *A*-site with different combinations of *B*-site elements. Sr_2MnMoO_6 [8] and Ba_2MnMoO_6 [23] represent *A*-site substitution with fixed *B*-site elements. From previous research, the electronic structure between Sr_2FeMoO_6 [4–8] and Sr_2CrMoO_6 [12,21] is similar, near the Fermi level, which gives a clue about the combination required for double perovskite HM compounds.

In order to find more potential HM materials, this paper presents theoretical HM compound prediction on double perovskites, $A_2BB'O_6$, by systematically substituting the *A*-site ion with fixed *BB'* combinations, such as Cr*M* (*M* = Mo, Re and W). For the *A*-site ion, the similarity of the valence electrons between the IVA group elements and alkaline-earth elements (Ca, Sr and Ba), denoted as IIA(s^2) and IVA(p^2), motivated us to use IVA group elements instead of alkaline-earth elements [24]. However, the elements in the IVA group are quite different from Sr, so an examination of the structural stability is still needed. All the compounds are stable, except the Si-based double perovskite structure. The double perovskite structure cannot be synthesized as the covalent bond of SiO_2, because the binding energy is too strong. Thus, calculations of density functional theory (DFT) were carried out, and new combinations of HM materials were found. The exempted HM materials in the preparation of this work are compounds of carbon, which represents the *A*-site position (C_2CrMO_6). This exemption is due to the covalent bounding of carbon, which is too strong. The valence of carbon is +4 rather than +2. For *M* = Mo and Re, all compounds can be HM materials, with Si_2CrMoO_6, Ge_2CrMo and Ge_2CrReO_6 needing strong correlation correction. For *M* = W, only *A* = Sn and Pb are possible candidates as HM materials.

2. Computational Method

The theoretical research is based on the calculation of first-principle DFT [25,26]. The exchange-correlation potential is formed by generalized gradient approximation (GGA) [27]. The full-potential projector augmented wave (PAW) [28] method is implemented in the VASP (The Vienna *ab-initio* Simulation Package) code [29,30], where the cut-off energy of the plane wave basis was set as

450 eV. The $8 \times 8 \times 6$ *k*-point grids were set in the Brillouin zone. The conjugate-gradient (CG) method was used to find the stable ionic positions, *i.e.*, this is the process of relaxation for both lattice constants and atomic positions, denoted as full structural optimization. The theoretical equilibrium structures were obtained when the forces and stress acting on all the atoms were less than 0.03 eV/Å and 0.85 kBar, respectively. The energy convergence criteria for self-consistent calculations were set to 10^{-6} eV. The Wigner-Seitz radius of the atom was set to 2.5, 2.1 and 1.4 a.u. for *A*-site atoms, $3d$ transition metals and oxygen, respectively.

In transition metal oxides, such as double perovskites, GGA (Gradient Approximation Functional) calculations are not sufficient for strong electron correlation systems. However, the GGA calculation can be corrected by using a strong correlation correction, called the GGA (LDA (Local Approximation Functional)) + *U* (Coulomb parameter) method [31,32], to fit in these systems. The GGA(LDA) + *U* scheme yields satisfying results for many strongly correlated systems, and it is a useful approach [33–35]. Thus, GGA + *U* calculations were performed in this work. The effective parameter $U_{eff} = U - J$ was adopted, where *U* and *J* stand for Coulomb and exchange parameters, respectively (we used *U* instead of U_{eff} for simplicity in this paper). The near-maximum values were selected from the reasonable range of *U* [36] in the transition metal. For example, the range of *U* for Cr is 1.5 eV to 3.0 eV. In this work, 3.0 eV is used in the calculation. The *U* values are listed in Table 1.

3. Results and Discussions

In an ordered double perovskite structure, $A_2BB'B_6$ (Figure 1), four magnetic phases exist: ferromagnetic (FM), ferrimagnetic (FiM), antiferrimagnetic (AF) and nonmagnetic (NM). These phases are controlled by the spin state of the two *B* and *B'* ions. In the ideal cubic structure ($Fm\overline{3}m$, no. 225) for FM and FiM states, the *B* and *B'* ions can be described in the order of the NaCl configuration, i.e., a face-centered cubic (fcc) stacked by *B* and *B'* ions with lattice constant $2a$. In the fcc cubic, each $B(B')$ is coordinated by $B'(B)$, and each has an O ion between, so there are 6 *B*-O-*B'* bonds per unit cell with the length of *B*-O and *B'*-O being equal. To determine theoretical lattice constants and atomic positions by structural optimization calculations, a larger unit cell with 2 f.u. (formula unit) was considered to enable the structure to relax to a reduced symmetry. [37] After full structural optimization, most of the ideal cubic structure ($Fm\overline{3}m$, no. 255) will reduce to a tetragonal ($I4/mmm$, no. 139) structure. In the tetragonal structure ($I4/mmm$), there are two nonequivalent types of O atoms, as shown in Table 2. There are two O_1 atoms located on the *z*-axis with *B* and *B'* atoms sitting between, and the four O_2 atoms are located on the *xy*-plane; the same as the *B* and *B'* atoms (Figure 1 and Table 2). The angle of the *B*-O-*B'* remained at 180° during structural optimization, whereas the lattice constant and bond length changed. The closeness of the c/a ratio to the ideal value, $\sqrt{2}$, shows that the symmetry reduction is minor. Although some compounds remained in the ideal cubic structure ($Fm\overline{3}m$, no. 255) during full structural optimization, the O_1 and O_2 are equivalent to the c/a ratio, $\sqrt{2}$. In the AF state, the tetragonal structure ($P4/mmm$, no. 123) remains the same in the full structural optimization.

Table 1. Calculated physical properties of the A_2CrMO$_6$ in a double perovskite structure in the full structural optimization calculation of generalized gradient approximation (GGA) + U (Coulomb parameter).

Materials A_2Cr[M]O$_6$	U (Cr, M)	Spin magnetic moment (μ$_B$/f.u.)			d Orbital electrons ↑/↓		$N(E_F)$ states/eV/f.u.	Band gap eV	Spin-polarization $N((↑−↓)/(↑+↓))$ (%)	ΔE = FM − AF meV/f.u.
		M_{Cr}	M_M	m_{tot}	Cr	M				
Si[Mo]	(0, 0)	2.297	−0.407	2.004	3.333/1.069	1.934/2.320	↑0.152/↓2.739		−89.5	−27.9
	(3, 2)	2.618	−0.701	2.000	3.479/0.898	1.764/2.442	↓3.620	↑0.925	−100.0	−197.9
Ge[Mo]	(0, 0)	2.318	−0.439	2.000	3.336/1.051	1.914/2.332	↓3.108	↑0.150	−100.0	−63.1
	(3, 2)	2.267	−0.729	2.000	3.474/0.885	1.746/2.451	↓3.592	↑1.100	−100.0	−109.3
Sn[Mo]	(0, 0)	2.370	−0.503	2.000	3.328/0.992	1.864/2.344	↓2.759	↑0.675	−100.0	−117.3
	(3, 2)	2.656	−0.806	2.000	3.447/0.829	1.690/2.471	↓3.143	↑1.675	−100.0	−118.1
Pb[Mo]	(0, 0)	2.381	−0.513	2.000	3.324/0.977	1.850/2.340	↓2.767	↑0.700	−100.0	−123.7
	(3, 2)	2.659	−0.806	2.000	3.439/0.818	1.680/2.461	↓3.160	↑1.825	−100.0	−120.8
Si[Re]	(0, 0)	2.294	−0.958	1.095	3.319/1.059	1.659/2.593	↑0.541/↓2.357		−62.7	−158.1
	(3, 2)	2.624	−1.364	1.000	3.463/0.877	1.446/2.783	↓2.243	↑1.125	−100.0	−176.3
Ge[Re]	(0, 0)	2.314	−1.030	1.042	3.323/1.043	1.623/2.628	↑0.338/↓4.108		−84.8	−253.9
	(3, 2)	2.631	−1.399	1.000	3.458/0.865	1.427/2.798	↓2.303	↑1.300	−100.0	−292.9
Sn[Re]	(0, 0)	2.360	−1.125	1.000	3.317/0.992	1.568/2.666	↓2.772	↑0.800	−100.0	−301.9
	(3, 2)	2.652	−1.469	1.000	3.433/0.819	1.384/2.824	↓2.842	↑1.850	−100.0	−276.3
Pb[Re]	(0, 0)	2.372	−1.143	1.000	3.314/0.977	1.553/2.669	↓2.865	↑0.875	−100.0	−308.7
	(3, 2)	2.656	−1.473	1.000	3.426/0.808	1.376/2.282	↓2.875	↑1.825	−100.0	−273.9
Si[W]	(0, 0)	2.377	−0.268	2.617	3.359/1.015	1.951/2.199	↑0.545/↓2.226		−60.7	−28.9
	(3, 2)	2.640	−0.429	2.165	3.464/0.861	1.826/2.235	↑0.550/↓2.300		−61.4	−53.6
Ge[W]	(0, 0)	2.374	−0.311	2.131	3.355/1.014	1.925/2.215	↑0.473/↓2.273		−65.5	−70.6
	(3, 2)	2.635	−0.496	2.119	3.458/0.859	1.790/2.625	↑0.438/↓2.449		−69.7	−85.6
Sn[W]	(0, 0)	2.349	−0.454	2.000	3.320/1.004	1.842/2.273	↓3.149	↑0.825	−100.0	−166.2
	(3, 2)	2.623	−0.703	2.000	3.422/0.834	1.683/2.360	↓3.177	↑1.900	−100.0	−143.2
Pb[W]	(0, 0)	2.352	−0.464	2.000	3.313/0.993	1.831/2.271	↓2.890	↑1.025	−100.0	−180.2
	(3, 2)	2.622	−0.716	2.000	3.411/0.825	1.671/2.360	↓3.099	↑2.725	−100.0	−151.9

FM, ferromagnetic; AF, antiferrimagnetic. (↑ and ↓ stand for the spin states).

Figure 1. An ideally ordered double perovskite structure, A_2CrMO_6.
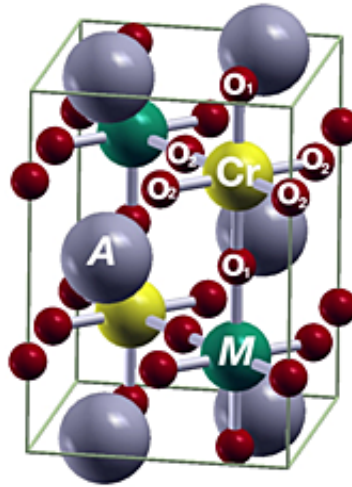
Table 2. Structural parameters in the fully optimized structure ($I4/mmm$, no. 139 and $Fm\overline{3}m$, no. 255), where A (x, y, z) = (0, 0.5, 0.75), Fe (x, y, z) = (0, 0, 0), M (x, y, z) = (0, 0, 0.5), O_1 (x, y, z) = (0, 0, O_{1z}) and O_2 (x, y, z) = (O_{2x}, O_{2y}, 0.5).

A_2Cr[M]O$_6$	a	c/a	V_0 (Å³/f.u.)	O_1z	O_2x	O_2y
Si[Mo]	5.4616	1.4138	115.17	0.24755	0.25238	0.25238
Ge[Mo]	5.4816	1.4135	116.41	0.24779	0.25210	0.25210
Sn[Mo] *	5.5653	$\sqrt{2}$	121.89	0.24896	0.24896	0.24896
Pb[Mo]	5.5879	1.4146	123.41	0.24923	0.25077	0.25077
Si[Re]	5.4561	1.4134	114.78	0.24926	0.25075	0.25075
Ge[Re]	5.4768	1.4136	116.11	0.24931	0.25071	0.25071
Sn[Re]	5.5614	1.3920	119.72	0.24974	0.25025	0.25025
Pb[Re] *	5.5837	$\sqrt{2}$	123.10	0.25000	0.25000	0.25000
Si[W]	5.4719	1.4137	115.80	0.24951	0.25047	0.25047
Ge[W]	5.4892	1.4147	116.99	0.24966	0.25038	0.25038
Sn[W] *	5.5721	$\sqrt{2}$	122.33	0.25059	0.25059	0.25059
Pb[W]	5.5952	1.4147	123.90	0.25109	0.24884	0.24884

The asterisk (*) represents the ideal cubic structure ($Fm\overline{3}m$) with the O$_1$ and O$_2$ equivalent.

The investigation of structural stability is necessary, because Si, Ge, Sn and Pb are quite different from Sr. The structural stability can be examined by the energy difference between the double perovskite structure and existing materials, such as $AO_{(2)}$ (A = Si, Ge, Sn and Pb), MO_2 (M = Mo, Re and W) and $CrO_{(2)}$. Thus, the energy difference can be written as Equations (1) and (2), where E_{tot}(f.u.) represents the energy of each compound.

$$\Delta E = E_{tot}\ (A_2FeMO_6) - [E_{tot}\ (AO_2) \times 2 + E_{tot}\ (CrO) + E_{tot}\ (MO)] \tag{1}$$

$$\Delta E = E_{tot}\ (A_2FeMO_6) - [E_{tot}\ (AO) \times 2 + E_{tot}\ (CrO_2) + E_{tot}\ (MO_2)] \tag{2}$$

SiO$_2$, GeO$_2$, SnO$_2$, PbO$_2$, SnO, PbO, CrO, CrO$_2$ and MO_2 are existing materials that can be easily calculated. The case of MO is a bit tricky, because MO_2 actually exists, but not MO. Thus, the energy of MO can be calculated by the average of MO_2 and M bulk, which can be expressed as:

$$E_{tot}\ (MO) = [E_{tot}\ (M) + E_{tot}\ (MO_2)] \times 0.5$$

<div align="right">(3)</div>

The result shows that all compounds are stable, except the Si-based double perovskite structure. The energy differences (ΔE) for Si, Ge, Sn and Pb of A_2CrMO_6 are 8 eV/f.u. to 10 eV/f.u., -0.5 eV/f.u. to -2 eV/f.u., -10 eV/f.u. to -12 eV/f.u., and -9 eV/f.u. to -13 eV/f.u., respectively. These results show that after oxidation, the crystal ionic radii for Si^{4+} are too small, so the bond of the electrons remains close to the Si^{4+} ion, thereby producing a covalent bond. The binding energy of SiO_2 (covalent bond) is too strong, such that the double perovskite structure cannot be synthesized. Sr_2FeMoO_6 is also stable. We present the Si-based double perovskite structure to ensure the integrity of our work.

In the FM and FiM states, the *B* and *B'* ions each have the same spin state, that is FM $(B, B, B', B') = (m, m, m', m')$ and FiM $(B, B, B', B') = (m, m, -m', -m')$, which can lead us to the assumption of the HM state. For the AF state, the spin state can be shown as $(B, B, B', B') = (m, -m, m', -m')$. The induced equivalence in the charges is $Q\uparrow [B\ (B')] = Q\downarrow [B\ (B')]$. In the total density of state (DOS), symmetrical spin-up and spin-down electron distribution can be observed, but no HM features are evident. In the NM phase, there is no spin polarization effect, which results in the absence of magnetic properties. To ascertain which magnetic phase is the most stable, calculations for all four magnetic phases are performed. The result shows that spin-polarized calculated total energies are always lower than those without spin-polarization and the initial FM and FiM state all converge to the FiM state. To guarantee the accuracy of the calculation result, a self-consistent process with higher convergence criteria is also performed.

Based on the energy difference in Table 1, the FiM state is the most stable magnetic phase in all compounds. In A_2CrMO_6, the half-metallic characteristics can be obtained by the energy gap at the spin-up channel with a total magnetic moment (m_{tot}) of 2.0, 1.0 and 2.0 μ_B for $M = $ Mo, Re and W in the GGA calculation, respectively. Except (1) for $M = $ Mo and Re, Si_2CrMoO_6, Ge_2CrMoO_6 and Ge_2CrReO_6 need a strong correlation correction (GGA + U), and (2) for $M = $ W. Only $A = $ Sn and Pb are possible candidates as HM materials. The lattice constant and volume of the unit cell will rise with the *A* site atom from silicon to lead (Table 2), and it will narrow down the electron band structure. The energy gap will appear and become larger (Table 1). The maintenance of the conductivity at the spin-down channel and the behavior between the size of the *A*-site ion and energy gap at the spin-up channel cause the success of $A = $ Sn and Pb as candidate HM materials. The IVA group elements near the top of the Periodic Table show their strong covalent characteristics. The ionic characteristics become stronger as we go deeper. The positive charge of the atomic nucleus will gain attraction to the inner shell (*s*-orbital) of valence electrons. Thus, the valence from C ($2s^2 2p^2$) to Pb ($6s^2 6p^2 \sim 6p^2$) can be denoted as +4 to +2, whereas the others are in between. Thus, IVA group elements, like Pb ($6p^2$), are similar to Sr ($5s^2$) in the outer valence electron. This is also the reason for the absence of half metallicity in the carbon stand for the *A* site in each compound. The value of the effective parameter, U (U_{Cr}, UM), is tuned up from (3, 2) to (5, 3). All results were the same: (1) in all compounds, the FiM magnetic phase is still the most stable state compared with the AF state by about 10^1 meV to 10^2 meV; and (2) the HM compound still carries its original characteristics, and the non-HM compound (Si_2CrWO_6, Ge_2CrWO_6) has no spin-polarized gap.

Figure 2 presents the density of states (DOS) of A_2CrMoO_6, A_2CrReO_6 and A_2CrWO_6 in GGA calculations. The electronic structures are very similar to each other in that they share the same mechanism of HM characteristics. Below the Fermi level (E_F), the O *2p* orbital extends from about

−8 eV to −2 eV, and hybrids with the M t_{2g} orbital are in the same energy region. The Cr t_{2g} orbital in the spin-up channel extends from about −6 eV to −3 eV, which hybrids with the O $2p$ orbital, and from −2 eV to −0.5 eV below E_F. With the M t_{2g} and Cr e_g orbitals above the E_F, the band gap appears at the spin-up channel. In the spin-down channel, the M t_{2g} orbital extends from about −1 eV to 1 eV, which dominates the conductivity of the whole compound. In the ionic picture, the formal valence of CrM is +8, and the electron configuration is Cr^{3+} ($t_{2g}^3 e_g^0$), S = 3/2; Mo^{5+} ($t_{2g}^1 e_g^0$), S = −1/2 for A_2CrMoO$_6$, and Cr^{3+} ($t_{2g}^3 e_g^0$), S = 3/2; Re^{5+} ($t_{2g}^2 e_g°$), S = −1 for A_2CrReO$_6$, and Cr^{3+} ($t_{2g}^3 e_g^0$), S = 3/2; W^{5+} ($t_{2g}^1 e_g^0$), S = −1/2 for A_2CrWO$_6$; according to the calculated electron numbers. The number of valence electrons for Re^{5+} ($t_{2g}^2 e_g^0$) is greater than that for Mo (W)$^{5+}$($t_{2g}^1 e_g^0$) by one, whereas the local magnetic moment of Re is about two times larger than that of Mo (W). The value of spin polarization is important for applications in spintronics, which can be defined as (N↑ − N↓)/(N↑ + N↓), where N denotes the spin-up (↑) and spin-down (↓) components in the DOS at the E_F. In all HM compounds of this work, spin polarizations are all −100%. The negative sign indicates that the metallic behavior can only be obtained in the spin-down channel. For other materials, they still show high spin polarization more than −65%, such as Si$_2$CrMoO$_6$ (−89.5%), Ge$_2$CrReO$_6$ (−84.8%) and Ge$_2$CrWO$_6$ (−65.5%) in the GGA scheme, indicating that they may still be applied in spintronics.

Figure 2. Calculated total, spin and site partial density of states in GGA of (**a**) A_2CrMoO$_6$; (**b**) A_2CrReO$_6$; and (**c**) A_2CrWO$_6$. DOS, density of states.
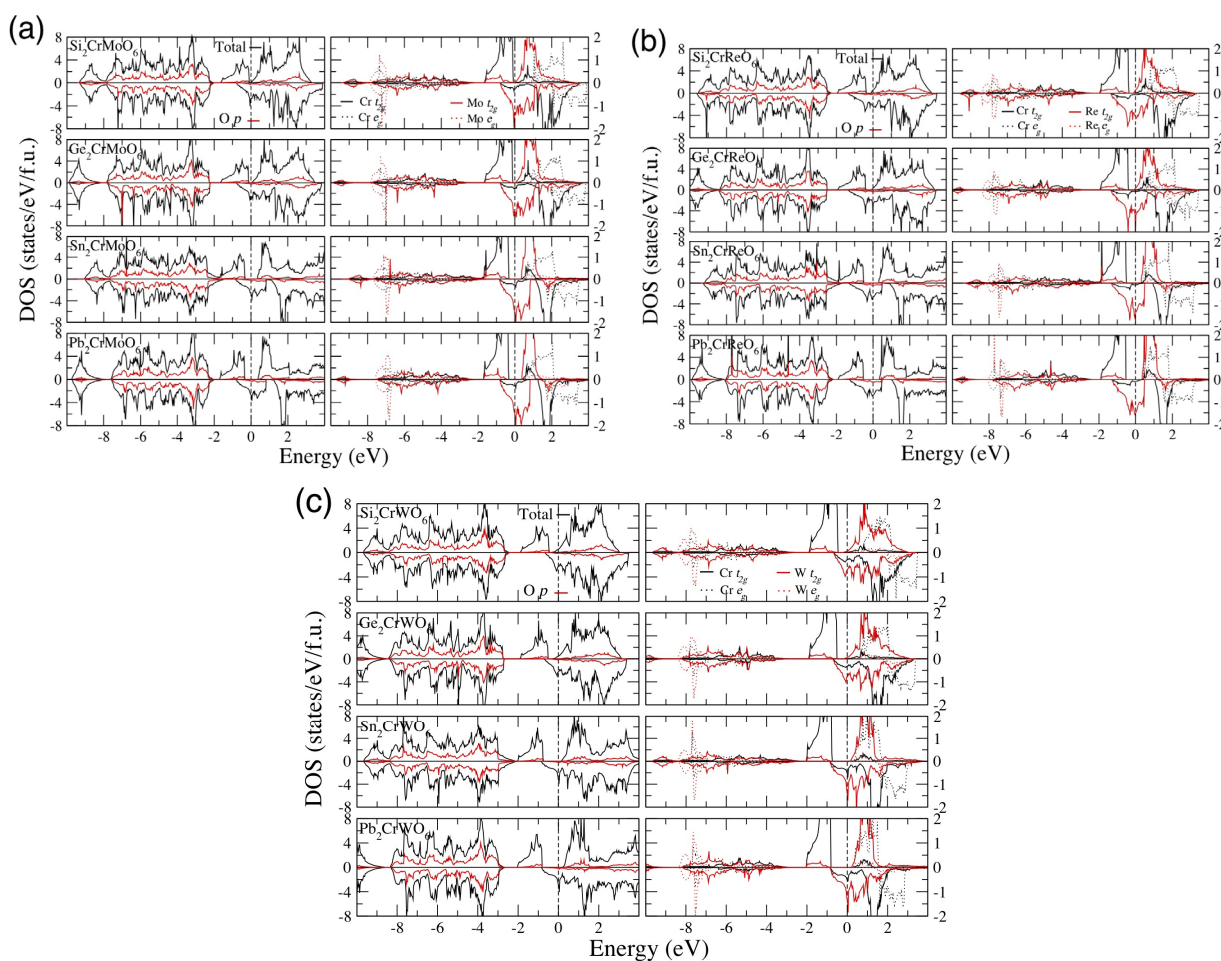
The exchange correlation correction effects (GGA + U) are similar in all compounds. Thus, we present the GGA + U calculations for Pb_2CrMO_6 (M = Mo, Re and W) in Figure 3. When the exchange correlation effect is induced, it will give rise to the electronic structure. For Pb_2CrMO_6, the Cr t_{2g} orbital is pushed down deeper, and all the orbitals become more localized, which enhances the local magnetic moment (LMM). Therefore, the band gap at the spin-up channel and the LMM becomes larger. For example, the band gap of Pb_2CrMO_6 grows from 0.70 (0.875, 1.03) eV to 1.83 (1.83, 2.73) eV for M = Mo (Re, W) in the GGA and GGA + U processes, respectively. The LMM improves from 2.381 (2.372, 2.352) to 2.659 (2.656, 2.622) for Fe and −0.513 (−1.143, −0.464) to −0.806 (−1.473, −0.716) for Mo (Re, W) in GGA and GGA + U, respectively. With the consideration of the exchange correlation effect, Si_2CrMoO_6, Ge_2CrMo and Ge_2CrReO_6 appear to be HM materials, where m_{tot} turned into an integer from 2.004, 1.095 and 1.042 μ_B to 2.0, 1.0 and 1.0 μ_B, respectively. Each opened a gap at the spin-up channel of 3.62, 2.24 and 2.303 eV, respectively (Table 1). However, for Si_2CrWO_6 and Ge_2CrWO_6, even the effective parameter, U (U_{Cr}, UM), tuned up from (3, 2) to (5, 3). The HM characteristic never appears.

Figure 3. Calculated total, spin and site partial density of states of Pb_2CrMO_6 (M = Mo, Re and W) in GGA + U (3, 2).
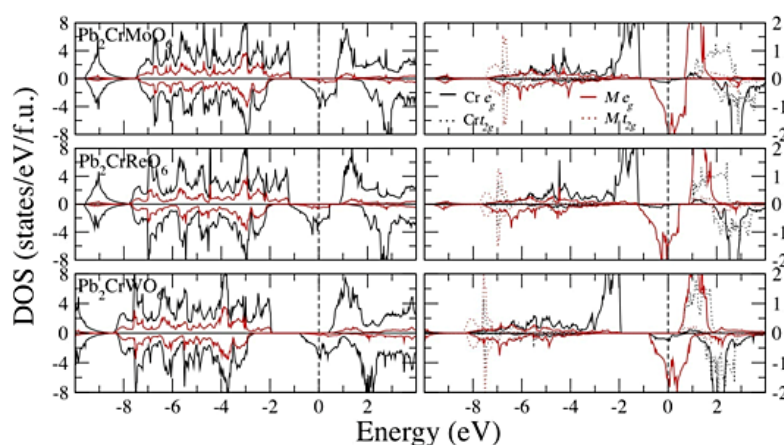
For the mechanism of the half metallicity and ferrimagnetic phase, Terakura *et al.* [38] proposed an F(i)M stabilization mechanism, while a nonmagnetic element is in between magnetic elements with the *p-d* hybridization and double exchange interaction. For example, magnetic elements with a full spin splitting orbital with the E_F located in the middle are denoted as *d*-states. The non-magnetic elements located at E_F and between the spin-polarized *d*-states are denoted as *p*-states. In the spin-up (down) channel, the *d*-state will push the *p*-state upward (downward). Thus, the E_F will be unequal in both spin states. To keep the E_F common, some electrons will switch spin states that move nonmagnetic elements to contribute negative moments and stabilize the F(i)M state. This phenomenon is called *p-d* hybridization. If such hybridization is strong enough, the *p*-state can be pushed above the E_F at one spin channel. With the double exchange effect, the band extends at the opposite spin channel with the E_F. Half metallicity and ferrimagnetic appear spontaneously. These behaviors do not exist in the AF configurations; thus, the FiM states are more stable than AF states. In our work, the Cr t_{2g} orbital represents the spin-split *d*-states. The M t_{2g} orbital stands for the *p*-state nonmagnetic elements, whereas weak-magnetic elements are also suitable for *p*-state elements.

4. Conclusions

In this paper, by granting that the valence electrons between IIA (s^2) and IVA (p^2) are similar, the IVA group elements on the *A*-site ion position instead of the alkaline-earth elements were attained in the double perovskite structure, $A_2BB'O_6$. The calculations of DFT were carried out with the fixed BB' combinations as Cr*M* (*M* = Mo, Re and W). The examination of structural stability revealed that all the compounds were stable, except Si-based double perovskite structures, such as that of Si_2CrMO_6. Thus, in A_2CrMO_6 (*A* = Ge, Sn, and Pb), with *M* = Mo and Re, all the compounds can be used as HM materials, except Ge_2CrMoO_6 and Ge_2CrReO_6, for which the GGA + *U* process is recommended. For *M* = W, only *A* = Sn and Pb are possible candidates as HM materials. The *p-d* hybridization between the Cr_d-M_p and the double exchange are the main reasons for the half metallicity and ferrimagnetic phase (HM-FiM). We hope this work helped in the identification of more candidate HM materials and will encourage further experimental research.

Conflicts of Interest

The authors declare no conflict of interest.

References

1. Longo, J.M.; Ward, R. Compounds of heptavalent rhenium with the perovskite structure. *J. Am. Chem. Soc.* **1961**, *83*, 1088–1090.
2. Garcia-Landa, B.; Ritter, C.; Ibarra, M.R.; Blasco, J.; Algarabel, P.A.; Mahendiran, R.; Garcia, J. Magnetic and magnetotransport properties of the ordered perovskite Sr_2FeMoO_6. *Solid State Commun.* **1999**, *110*, 435–438.
3. Jin, S.; Teifel, T.H.; McCormack, M.; Fastacht, R.A.; Ramesh, R.; Chen, L.H. Thousandfold change in resistivity in magnetoresistive La-Ca-Mn-O films. *Science* **1994**, *264*, 413–415.
4. Kobayashi, K.I.; Kimura, T.; Sawada, H.; Terakura, K.; Tokura, Y. Room-temperature magnetoresistance in an oxide material with an ordered double-perovskite structure. *Nature* **1998**, *395*, 677–680.
5. Kobayashi, K.I.; Kimura, T.; Tomioka, Y.; Sawada, H.; Terakura, K.; Tokura, Y. Intergrain tunneling magnetoresistance in polycrystals of the ordered double perovskite Sr_2FeReO_6. *Phys. Rev. B* **1999**, *59*, 11159.

6. Chan, T.S.; Liu, R.S.; Guo, G.Y.; Hu, S.F.; Lin, J.G.; Chen, J.M.; Chang, C.-R. Effects of B'-site transition metal on the properties of double perovskites Sr_2FeMO_6 (M = Mo, W): B' 4d–5d system. *Solid State Commun.* **2005**, *133*, 265–270.

7. Moritomo, Y.; Kusura, H.; Akimoto, T.; Machida, A. Room-Temperature Magnetoresistance in Fe-Site-Substituted Sr_2FeMoO_6. *Jpn. J. Appl. Phys.* **2000**, *39*, L360–L362.

8. Itoh, M.; Ohta, I.; Inaguma, Y. Cooperative interaction of oxygen octahedra for dielectric properties in the perovskite-related layered compounds $Sr_{n+1}TinO_{3n+1}$, $Ca_{n+1} TinO_{3n+1}$ and $Sr_{n+1}(Ti_{0.5}Sn_{0.5})_nO_{3n+1}$ (n = 1,2,3 and ∞). *Mater. Sci. Eng. B* **1996**, *41*, 50–54.

9. Cheng, J.; Yang, Z.Q. Electronic structures of double perovskites Ba_2MnMO_6 (M = W and Re) from first-principles studies. *Phys. Status. Solidi B* **2006**, *243*, 1151–1158.

10. Gray, B.; Lee, H.N.; Liu, J.; Chakhalian, J.; Freeland, W. Local electronic and magnetic studies of an artificial La_2FeCrO_6 double perovskite. *Appl. Phys.Lett.* **2010**, *97*, 013105.

11. Tang, C.Q.; Zang, Y.; Dai, J. Electronic and magnetic structure studies of double perovskite Sr_2CrReO_6 by first-principles calculations. *Solid State. Commun.* **2005**, *133*, 219–222.

12. Wu, H. Electronic structure study of double perovskites A_2FeReO_6 (A = Ba,Sr,Ca) and Sr_2MMoO_6 (M = Cr,Mn,Fe,Co) by LSDA and LSDA + U. *Phys. Rev. B* **2001**, *64*, 125126.

13. Sarma, D.D.; Mahadevan, P.; Dasgupta, T.S.; Ray, S.; Kumar, A. Electronic structure of Sr_2FeMoO_6. *Phys. Rev. Lett.* **2000**, *85*, 2549–2554.

14. Jeng, H.T.; Guo, G.Y. First-principles investigations of orbital magnetic moments and electronic structures of the double perovskites Sr_2FeMoO_6, Sr_2FeReO_6, and Sr_2CrWO_6. *Phys. Rev. B* **2003**, *67*, 1–4.

15. Kato, H.; Okuda, T.; Okimoto, Y.; Tomioka, Y. Structural and electronic properties of the ordered double perovskites A_2MReO_6 (A = Sr, Ca; M = Mg, Sc, Cr, Mn, Fe, Co, Ni, Zn). *Phys. Rev. B* **2004**, *69*, 184412.

16. Solovyev, I.V. On the competition between ferromagnetic and antiferromagnetic states in Sr_2MnMoO_6. *J. Magn. Magn. Mater.* **2004**, *268*, 194–197.

17. Song, W.; Wang, J.; Wu, Z. Half metallic properties of Sr_2CuOsO_6. *Chem. Phys. Lett.* **2009**, *482*, 246–248.

18. Wang, J.; Wang, J.; Wu, Z. First principles investigations on the half metallic properties of Sr_2MOsO_6 (M = V, Mn, Fe, Co). *Chem. Phys. Lett.* **2011**, *501*, 324–329.

19. Yousif, S.E.A.; Yassin, O.A. The electronic and magnetic properties of Sr_2MnNbO_6, Sr_2FeMoO_6 and Sr_2NiRuO_6 double perovskites: An LSDA + U + SOC study. *J. Alloys Compd.* **2010**, *506*, 456–460.

20. Bannikov, V.V.; Shein, I.R.; Kozhevnikov, V.L.; Ivanovsky, A.L. Electronic structure and magnetic properties of double perovskites Sr_2FeMO_6 (M = Sc, Ti, ..., Ni, Cu) according to the data of FLAPW-GGA band structure calculations. *J. Struct. Chem.* **2008**, *49*, 781–787.

21. Bonilla, C.M.; Landínez Téllez, D.A.; Arbey Rodríguez, J.; Vera López, E.; Roa-Rojas, J. Half-metallic behavior and electronic structure of Sr_2CrMoO_6 magnetic system. *Phys. B* **2007**, *398*, 208–211.

22. Philipp, J.B.; Majewski, P.; Alff, L.; Erb, A.; Gross, R.; Graf, T.; Brandt, M.S.; Simon, J.; Walther, T.; Mader, W.; *et al*. Structural and doping effects in the half-metallic double perovskite A_2CrWO_6 (A = Sr, Ba, and Ca). *Phys. Rev. B* **2003**, *68*, 144431.

23. Liu, Y.P.; Fuh, H.R.; Wang, Y.K. First-principles study of half-metallic materials in double-perovskite A_2FeMO_6 (M = Mo, Re, and W) with IVA group elements set on the A-site position. *J. Phys. Chem. C* **2012**, *116*, 18032–18037.

24. Cardona, R.; Landínez Téllez, D.A.; Arbey Rodríguez M., J.; Fajardo, F.; Roa-Rojas, J. Structural and magnetic properties of double-perovskite Ba_2MnMoO_6 by density functional theory. *J. Magn. Magn. Mater.* **2008**, *320*, e85–e87.

25. Hohenberg, P.; Kohn, W. Inhomegeneous electron gas. *Phys. Rev.* **1964**, *136*, B864.

26. Kohn, W.; Sham, L.J. Self-Consistent equations including exchange and correlation effects. *Phys. Rev.* **1965**, *140*, A1133.

27. Blöchl, P.E. Projector augmented-wave method. *Phys. Rev. B* **1994**, *50*, 17953.

28. Perdew, J.P.; Burke, K.; Ernzerhof, M. Generalized Gradient Approximation Made Simple. *Phys. Rev. Lett.* **1996**, *77*, 3865.

29. Kresse, G.; Hafner, J. *Ab initio* molecular dynamics for open-shell transition metals. *Phys. Rev. B* **1993**, *48*, 13115.

30. Kresse, G.; Furthmüller, J. Efficient iterative schemes for *ab initio* total-energy calculations using a plane-wave basis set. *Phys. Rev. B* **1996**, *54*, 11169.

31. Anisimov, V.I.; Zaanen, J.; Andersen, O.K. Band theory and Mott insulators: Hubbard U instead of Stoner I. *Phys. Rev. B* **1991**, *44*, 943.

32. Lichtenstein, A.I.; Anisimov, V.I.; Zaanen, J. Density-functional theory and strong interactions: Orbital ordering in Mott-Hubbard insulators. *Phys. Rev. B* **1995**, *52*, R5467.

33. Anisimov, V.I.; Aryasetiawan, F.; Lichtenstein, A.I. First-principles calculations of the electronic structure and spectra of strongly correlated systems: the LDA + U method. *J. Phys* **1997**, *9*, 767.

34. Jeng, H.T.; Guo, G.Y.; Huang, D.J. Charge-orbital ordering and verwey transition in magnetite. *Phys. Rev. Lett.* **2004**, *93*, 156403.

35. Jiang, X.; Guo, G.Y. Electronic structure and exchange interactions in BaVS3. *Phys. Rev. B* **2004**, *70*, 035110.

36. Solovyev, I.V.; Dederichs, P.H.; Anisimov, V.I. Corrected atomic limit in the local-density approximation and the electronic structure of d impurities in Rb. *Phys. Rev. B* **1994**, *50*, 16861.

37. Wang, Y.K.; Lee, P.H.; Guo, G.Y. Half-metallic antiferromagnetic nature of La_2VTcO_6 and La2VCuO6 from *ab initio* calculations. *Phys. Rev. B* **2009**, *80*, 224418.

38. Terakura, K.; Fang, Z.; Kanamori, J. High pressure phase transition and elastic properties of cerium chalcogenides and pnictides. *J. Phys. Chem. Solids* **2002**, *63*, 907–912.